Genetic Variation for Ontogenetic Shifts in Metabolism Underlies Physiological Homeostasis in *Drosophila*

Omera B. Matoo,[1] Cole R. Julick, and Kristi L. Montooth
School of Biological Sciences, University of Nebraska-Lincoln, Nebraska 68502
ORCID ID: 0000-0001-9456-6694 (K.L.M.)

ABSTRACT Organismal physiology emerges from metabolic pathways and subcellular structures like the mitochondria that can vary across development and among individuals. Here, we tested whether genetic variation at one level of physiology can be buffered at higher levels of biological organization during development by the inherent capacity for homeostasis in physiological systems. We found that the fundamental scaling relationship between mass and metabolic rate, as well as the oxidative capacity per mitochondria, changed significantly across development in the fruit fly *Drosophila*. However, mitochondrial respiration rate was maintained at similar levels across development. Furthermore, larvae clustered into two types—those that switched to aerobic, mitochondrial ATP production before the second instar, and those that relied on anaerobic, glycolytic production of ATP through the second instar. Despite genetic variation for the timing of this metabolic shift, metabolic rate in second-instar larvae was more robust to genetic variation than was the metabolic rate of other instars. We found that larvae with a mitochondrial-nuclear incompatibility that disrupts mitochondrial function had increased aerobic capacity and relied more on anaerobic ATP production throughout development relative to larvae from wild-type strains. By taking advantage of both ways of making ATP, larvae with this mitochondrial–nuclear incompatibility maintained mitochondrial respiratory capacity, but also had higher levels of whole-body reactive oxygen species and decreased mitochondrial membrane potential, potentially as a physiological defense mechanism. Thus, genetic defects in core physiology can be buffered at the organismal level via physiological plasticity, and natural populations may harbor genetic variation for distinct metabolic strategies in development that generate similar organismal outcomes.

KEYWORDS development; mtDNA; metabolism; oxidative phosphorylation; reactive oxygen species

METABOLISM is the sum total of biochemical processes that organisms use to sustain life and fuel reproduction, and an individual's metabolic rate is often interpreted as an integrated measure of its "pace of life" (Glazier 2005, 2014, 2015). Early surveys of natural molecular variation revealed a surprising amount of variation at loci encoding these biochemical processes (Harris 1966; Hubby and Lewontin 1966; Lewontin and Hubby 1966)—a pattern that has been historically used to advocate both for the predominance of classical mutation, drift, and purifying selection forces (Kimura 1983), and for the maintenance of variation through selection (Gillespie 1999; reviewed by Charlesworth and Charlesworth 2016). Subsequent surveys revealed substantial quantitative genetic variation in metabolic enzyme activities within species, arising from molecular variation at enzyme-encoding loci, as well as *trans*-acting and epistatic variation throughout the genome (Laurie-Ahlberg *et al.* 1980, 1982; Clark *et al.* 1995a,b; Clark and Wang 1997; Mitchell-Olds and Pedersen 1998; Montooth *et al.* 2003). In a few cases, this biochemical variation has been linked to variation at higher levels of physiological performance (Laurie-Ahlberg *et al.* 1982; Watt *et al.* 1983; Montooth *et al.* 2003; Crawford and Oleksiak 2007), and, in some cases, may be adaptive (Watt 1977; Tishkoff *et al.* 2001; Verrelli and Eanes 2001; Watt *et al.* 2003). However, we lack a mechanistic understanding of how genetic variation in the pathways of metabolism is transformed up the hierarchical

doi: https://doi.org/10.1534/genetics.119.302052
Manuscript received February 25, 2019; accepted for publication April 4, 2019; published Early Online April 11, 2019.
Available freely online through the author-supported open access option.
Supplemental material available at FigShare: https://doi.org/10.25386/genetics.7946795.
[1]Corresponding author: University of Nebraska-Lincoln, 1104 T St., Manter Hall, Lincoln, NE 68588-0118. E-mail: omatoo2@unl.edu

levels of biological organization to result in variation in organismal performance traits that determine fitness. This is important for consideration of metabolism as an adaptive phenotype and for predicting how selection on metabolic performance will shape variation in genomes.

A challenge to connecting genetic variation in biochemical processes to metabolic performance, is that metabolism is an emergent property of interacting biochemical, structural, regulatory, and physiological systems, often arranged in hierarchical functional modules (Jeong *et al.* 2000; Strogatz 2001; Ravasz *et al.* 2002; Barabási and Oltvai 2004). In addition, metabolic enzymes and metabolites have potential "moonlighting" functions in the signaling that underlies metabolic homeostasis (Marden 2013; Boukouris *et al.* 2016). The capacity for homeostasis in physiological systems also suggests that genetic variation in biochemical processes may not necessarily result in organismal fitness variation. The regulatory processes that maintain energy homeostasis may provide stability in metabolic trajectories in an analogous way to the canalized developmental trajectories envisioned by Waddington (1942, 1957) and Meiklejohn and Hartl (2002). Furthermore, multiple biochemical pathways may be available to achieve similar energetic outputs. Finally, the hierarchical biological processes that contribute to metabolism are influenced by both extrinsic (*e.g.*, temperature, resource availability, habitat) and intrinsic (*e.g.*, genotype, life stage, sex, reproductive status) factors (reviewed by Glazier 2005), such that genetic variation in biochemical processes may affect organismal performance and fitness in only a subset of conditions. Such conditionally neutral variation is expected to experience less effective selection (Van Dyken and Wade 2010).

Development is a potentially important context for the expression of genetic variation in metabolism. During development, organisms partition resources between the competing demands of growth, development, maintenance, and storage for future reproduction. Energy homeostasis during development is largely achieved by feedback controls where energy-demand processes increase the concentration of ADP, which is then available for energy-supply processes to generate ATP. The mitochondria play a central role in the energy supply-demand balance. Not only the abundance and activity of mitochondria, but also the surface area, membrane composition, and network structure of mitochondria have been reported to affect metabolism (Porter and Brand 1993; Porter *et al.* 1996; Miettinen and Björklund 2017). Oxidative phosphorylation (OXPHOS), which drives aerobic ATP production, requires proteins from both the mitochondrial and nuclear genomes, creating the potential for intergenomic epistasis to underlie variation in metabolic phenotypes. Our understanding of the underlying genetic architecture of metabolism is incomplete, but studies indicate that both nuclear DNA (nDNA) (Montooth *et al.* 2003; Nespolo *et al.* 2007; Tieleman *et al.* 2009), mitochondrial DNA (mtDNA) (Martin 1995; Ballard and Rand 2005; Arnqvist *et al.* 2010; Kurbalija Novičić *et al.* 2015), and interactions between genomes and environment affect metabolism (Hoekstra *et al.* 2013, 2018).

Energy balance is particularly challenging for holometabolous species with rapid and massive larval growth that requires simultaneous accumulation of the resources needed to fuel metamorphosis. *Drosophila melanogaster* is an especially powerful system to study developmental metabolism, given the genetic resources and an ~200-fold increase in body mass across three larval instars (Church and Robertson 1966). There is evidence of significant genetic variation for metabolic rate within *Drosophila* (Montooth *et al.* 2003; Hoekstra *et al.* 2013), and individuals with mitochondrial–nuclear genotypes that disrupt mitochondrial function have increased larval metabolic rate and delayed development (Hoekstra *et al.* 2013; Meiklejohn *et al.* 2013). Transcriptomic and metabolic profiling in *D. melanogaster* reveal the dynamic nature of energy metabolism that draws on both aerobic and anaerobic energy production, as well as the presence of proliferative metabolic programs during larval development (Graveley *et al.* 2011; Tennessen *et al.* 2011). Despite this wealth of data, we lack a detailed understanding of the links between genome variation, mitochondrial function, and organismal metabolic rate during development in *Drosophila*.

In the present study, we tested whether metabolic strategies in *D. melanogaster* varied across larval instars, using both wild-type larvae and larvae with a mitochondrial-nuclear genotype that compromises mitochondrial function. We observed significant variation in the ontogeny of metabolism at the level of mitochondrial aerobic capacity and ATP production, but also observed that this variation was buffered at higher levels of metabolic performance via physiological plasticity. Thus, there may be multiple genotypic and physiological paths to equivalent organismal outcomes within populations.

Methods

Drosophila stocks and maintenance

We used four *Drosophila* mitochondrial-nuclear (hereafter referred to as mito-nuclear) genotypes generated by Montooth *et al.* (2010). Individuals with the (*mtDNA*);-*nuclear* genotype (*simw*^{501});*OreR* have a genetic incompatibility that decreases OXPHOS activity putatively via compromised mitochondrial protein translation, resulting in delayed development, decreased immune function, and reduced female fecundity (Hoekstra *et al.* 2013, 2018; Meiklejohn *et al.* 2013; Holmbeck *et al.* 2015; Zhang *et al.* 2017; Buchanan *et al.* 2018). The mito-nuclear incompatibility is between naturally occurring single nucleotide polymorphisms (SNPs) in the mt-tRNA^{Tyr} gene and the nuclear-encoded mt-tyrosyl-tRNA synthetase gene *Aatm* that aminoacylates the mt-tRNA^{Tyr} (Meiklejohn *et al.* 2013). Individuals with the mito-nuclear genotypes—(*ore*);-*OreR*, (*simw*^{501});*Aut*, and (*ore*);*Aut*—serve as genetic controls that enable us to test for the effects of mitochondrial and nuclear genotypes, and their interaction on developmental physiology. Additionally, we measured traits in two inbred

isofemale fly strains sampled in Vermont (*VT4* and *VT10*) as representatives of natural populations that were not manipulated to generate specific mito-nuclear genotypes (for details see Cooper *et al.* 2014).

Flies from all strains were raised on standard cornmeal-molasses-yeast *Drosophila* medium and acclimated to 25° with a 12:12 hr dark:light cycle for at least three generations prior to all experiments. To collect first-, second- and third-instar larvae, adults were allowed to lay eggs for 3–4 hr on standard media, and larvae from these cohorts were staged based on developmental time and distinguishing morphological features.

Larval metabolic rate

Routine metabolic rate was measured as the rate of CO_2 produced by groups of 20 larvae of the same instar and strain using a flow-through respirometry system (Sable Systems International, Henderson, NV) (Hoekstra *et al.* 2013). Groups of larvae were collected onto the cap of 1.7 ml tube containing 0.5 ml of fly medium and placed inside one of four respirometry chambers that were housed in a temperature-controlled cabinet (Tritech Research, Los Angeles, CA) maintained at 25°. Between 8 and 13 biological replicates for each strain and instar were randomized across chambers and respirometry runs, during which each group of larvae was sampled for CO_2 production for two 10-min periods. CO_2 that accumulated in the chambers as a result of larval metabolism was detected using an infrared CO_2 analyzer (Li-Cor 7000 CO_2/H_2O Analyzer; LI-COR, Lincoln, NE). $\dot{V}CO_2$was calculated from the mean fractional increase in CO_2 at a constant air-flow rate of 100 ml/min over a 10-min time interval for each replicate after baseline-drift correction. The wet weight of the group of larvae was recorded using a Cubis microbalance (Sartorius AG, Göttingen, Germany) at the beginning of each respirometry run.

Larval water and lipid content

We measured larval whole-body water content using a protocol modified from Grefen *et al.* (2006). Six groups of 10 larvae each were collected for each strain at each instar, rinsed with larval wash buffer (0.7% NaCl and 0.1% Triton X-100), and blotted dry. The wet weight of the group of larvae was recorded ($\pm$0.01 mg) using a Cubis microbalance (Sartorius AG, Göttingen, Germany). Larvae were dried at 60° overnight and reweighed. The mass of whole-body water was calculated by subtracting dry mass from wet mass.

Larval whole-body lipid content was measured using a protocol modified from Bligh and Dyer (1959). Six groups of 10 larvae each were collected for each strain at each instar, rinsed with larval wash buffer, blotted dry, and weighed ($\pm$0.01 mg). Larvae were homogenized in a chloroform/methanol mixture (2:1 v/v) using tissue:solvent proportion of 1:20 w/v. Samples were sonicated for 1 min using a Sonic Dismembrators (ThermoFisher Scientific), vortexed for 1 hr at room temperature, and then centrifuged for 5 min at 13,000 $\times$ *g*. The supernatant was transferred in a new tube, mixed with ultrapure water (0.25 vol of the supernatant), vortexed for 2 min, and centrifuged for 5 min at 13,000 $\times$ *g*. The lower phase (chloroform) was transferred into a pre-weighed microcentrifuge tube and chloroform was allowed to evaporate to determine the dry mass of extracted lipids using a microbalance.

Isolation of mitochondria

Mitochondria were isolated from larvae following a protocol modified from Aw *et al.* (2016); 100–200 larvae for each biological replicate were collected and rinsed with larval wash buffer (0.7% NaCl and 0.1% Triton X-100). Larvae were gently homogenized in 300–500 μl of chilled isolation buffer (154 mM KCl, 1 mM EDTA, pH 7.4) in a glass-teflon Thomas® homogenizer on ice. The homogenate was filtered through a nylon cloth into a clean, chilled, microcentrifuge tube. The homogenate was then centrifuged at 1500 $\times$ *g* for 8 min at 4°. The resulting mitochondrial pellet was suspended in 40–50 μl of ice-cold mitochondrial assay solution (MAS: 15 mM KCl, 10 mM KH_2PO_4, 2 mM $MgCl_2$, 3 mM HEPES, 1 mM EGTA, FA-free BSA 0.2%, pH 7.2). Unless otherwise stated, all chemicals were purchased from Sigma Aldrich (St Louis, MO) or Fisher Scientific (Pittsburgh, PA) and were of reagent grade or higher.

Mitochondrial respiration

Oxygen consumption of freshly isolated mitochondria was measured using the Oxygraph Plus System (Hansatech Instruments, Norfolk, UK) in 3 ml water-jacketed glass chambers equipped with a magnetic stirrer and Clark-type oxygen electrodes. Temperature of the respiration chambers was kept constant at 25° using a Fisher Isotemp 4100 R20 refrigerated water circulator (Fisher Scientific, Hampton, NH). A two-point calibration of electrodes using air-saturated distilled water and sodium sulfite was done for establishing 100% and zero oxygen levels in the chamber, respectively. The assay was completed within 2 hr of mitochondrial isolation, and six or seven biological replicates were measured for each larval stage of each strain. Mitochondrial suspension (50 μl; $\sim$1.5 mg protein) was added to 950 μl of MAS in the respiration chamber. Pyruvate (5 mM) and malate (2.5 mM) were used as respiratory substrates at saturating amounts. Maximum respiration (State 3) was achieved by adding 400 μM of ADP, and State 4_{ol} respiration was calculated as described by Chance and Williams (1955) by adding 2.5 μg ml^{-1} oligomycin. Oligomycin is an ATPase inhibitor and State 4_{ol} gives an estimate of oxygen consumption linked to mitochondrial proton leak, rather than to ATP production, at high membrane potential (Brand *et al.* 1994). Uncoupled respiration (State 3u), indicative of maximum respiration or electron transport system (ETS) capacity, is achieved by adding 0.5 μM of carbonyl cyanide m-chlorophenyl hydrazone (CCCP). CCCP is a protonophore that increases proton permeability in mitochondria and effectively disconnects ETS from ATPase. Data were acquired and respiration rates were corrected for electrode drift using the OxyTrace$^+$

software. The respiratory control ratio (RCR^+) was calculated as the ratio of State 3 over State 4_{ol} (Estabrook 1967). Respiration rates were normalized by unit mitochondrial protein added. Protein concentrations were determined using Bio-Rad Protein Assay Dye Reagent Concentrate (5000006; Bio-Rad) and bovine serum albumin (BSA) as a standard.

Mitochondrial membrane potential ($\Delta\Psi_m$)

Mitochondrial membrane potential was measured using the JC-1 indicator dye (Fisher Scientific) following a protocol modified from Villa-Cuesta *et al.* (2014); 100 mg of larvae were weighed and used to isolate mitochondria as described above. Approximately 1.4 mg of mitochondrial protein was added, and the final volume was increased to 300 μl using MAS. Next, 3 μl of a 1 μg/μl solution of JC-1 dissolved in dimethyl sulfoxide (DMSO) was added to the suspension. Mitochondrial samples were incubated for 30 min at 37° protected from light. At the end of incubation, samples were centrifuged for 3 min at 6000 × *g* and suspended in 600 μl of fresh MAS. Mitochondrial membrane potential was expressed as the ratio of fluorescence for aggregate:monomeric forms of JC-1 at red (excitation 485 nm, emission 600 nm) and green (excitation 485 nm, emission 530 nm) wavelengths respectively; 50 μM of CCCP was added to collapse membrane potential as a negative control.

Citrate synthase activity

Citrate synthase activity was measured following the protocol from Meiklejohn *et al.* (2013); 100–200 larvae were homogenized in 1 ml chilled isolation buffer (225 mM mannitol, 75 mM sucrose, 10 mM MOPS, 1 mM EGTA, 0.5% fatty acid-free BSA, pH 7.2) using a glass-teflon Thomas® homogenizer. The homogenate was centrifuged at 300 × *g* for 5 min at 4°. The supernatant was transferred into a clean tube and centrifuged again at 6000 × *g* for 10 min at 4°. The resulting mitochondrial pellet was resuspended in 50 μl of respiration buffer (225 mM mannitol, 75 mM sucrose, 10 mM KCl, 10 mM Tris-HCl, and 5 mM KH_2PO_4, pH 7.2). All samples were stored at −80° till further analysis.

Maximum citrate synthase activity (V_{max}) of the mitochondrial extracts was measured spectrophotometrically at 25° using a Synergy 2 plate reader (BioTek); 6 μg of mitochondrial protein was added to the assay mixture containing 100 mM Tris-HCl (pH 8.0), 2.5 mM EDTA, 100 μM Acetyl Co-A, and 100 μM of DTNB [5,5′-dithiobis (2-nitrobenzoic acid)]. The reaction was monitored for 2 min as a background reading. The reaction was then started by adding 500 μM oxaloacetate to the assay to generate CoA-SH. CoA-SH was detected by its reaction with DTNB to form a yellow product (mercaptide ion) that was measured using absorbance at 412 nm. Enzyme activity was normalized by protein concentration of the sample added. Six biological samples per strain and instar were measured, each with two technical replicates.

Lactate quantification

Whole-body lactate concentrations were measured by an NAD^+/NADH-linked fluorescent assay following the protocol of Callier *et al.* (2015); 100–200 larvae were homogenized in 100–500 μl of 17.5% perchloric acid and centrifuged at 14,000 × *g* for 2 min at 4°. Following precipitation of proteins, the clear supernatant was transferred into a clean tube and neutralized with a buffer containing 2 M KOH and 0.3 M MOPS, and again centrifuged at 14,000 × *g* for 2 min at 4°. Neutralized sample (20–50 μl) was added to the assay buffer (pH 9.5) containing a final concentration of 1000 mM hydrazine, 100 mM Tris-base, 1.4 mM EDTA, and 2.5 mM NAD^+ in a 96-well plate. The assay was performed in fluorescence mode (Ex/Em = 360/460 nm) using a Synergy ^{1}H Hybrid Reader (BioTek). After incubating the plate for 5 min at room temperature, a background reading was taken. Lactate dehydrogenase (17.5 U/well; L3916; Sigma) diluted with Tris buffer was then added to each sample, and the reaction mixture was allowed to incubate at 37° for 30 min protected from light. A second reading was taken to measure NADH levels, after correcting for background fluorescence. Six biological samples per strain and instar were measured, each with two technical replicates. Sodium lactate was used as a standard for the assay. Lactate concentrations in the samples were normalized by the wet weight of the larvae.

Hydrogen peroxide quantification

Larvae (100–200) were weighed, rinsed with larval wash buffer (0.7% NaCl and 0.1% Triton X-100), and homogenized in 500 μl of prechilled assay buffer (pH 7.5) containing 20 mM HEPES, 100 mM KCl, 5% glycerol, 10 mM EDTA, 0.1% Triton X-100, 1 mM PMSF (P7626; Sigma), and 1:10 (v/v) protease inhibitor cocktail (P2714; Sigma) using a glass-teflon Thomas homogenizer. The homogenate was centrifuged at 200 × *g* for 5 min at 4°, and the supernatant was stored at −80°. Hydrogen peroxide (H_2O_2) concentration was determined with a fluorometric H_2O_2 Assay Kit (MAK 165; Sigma) following the manufacturer's protocol in a 96-well plate using the Synergy H1 Hybrid Reader. Six biological samples per strain and instar were measured, each with two technical replicates. H_2O_2 concentrations in the samples were expressed as nM/μg of protein. The mitochondria serve as both source and sink of reactive oxygen species (ROS) in the organism (Munro and Treberg 2017). Thus, we used this whole-body measure of H_2O_2 as an estimate of the organismal consequences of mitochondrial function.

Statistical analyses

All statistical analyses used the statistical package R version 2.15.1 (R Development Core Team 2011). We implemented standard major-axis regression in the R-package SMATR (Warton *et al.* 2006; Hoekstra *et al.* 2013) to estimate the relationship between log-transformed mass and $\dot{V}CO_2$, and to test for larval-instar and genetic effects on the slope of this relationship. When there was statistical evidence for a common slope among genotypes or strains, we fit the common

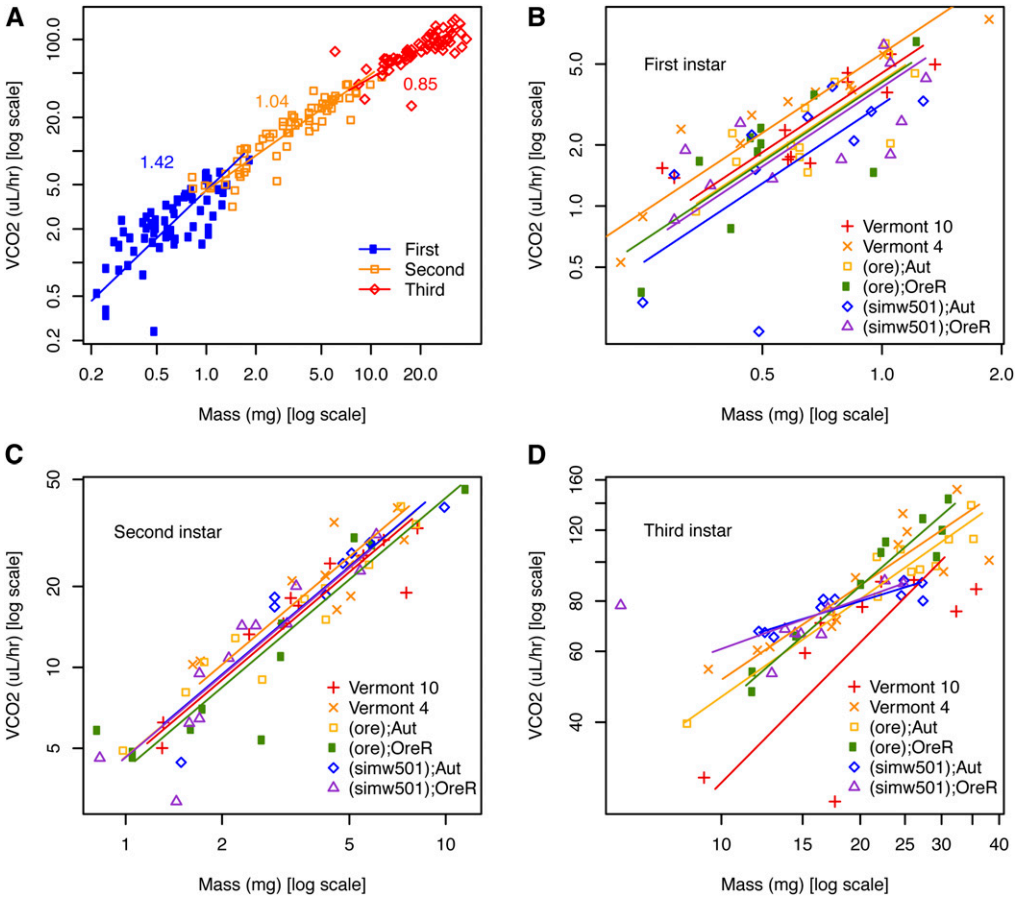

Figure 1 Metabolic scaling with mass varied across larval development and among strains. (A) The mass-scaling exponent for routine metabolic rate ($\dot{V}CO_2$) differed significantly among larvae from different instars (LR = 18.1, df = 2, P = 0.0001), with the relationship between metabolic rate and mass becoming more shallow across development. (B and C) There was more genetic variation for metabolic rate in first-instar larvae, relative to second-instar larvae. (D) Mass-scaling exponents differed significantly among strains in the third instar of development (Table 1 and Table S1).

slope to test for effects of genotype or strain on the y-intercept (*i.e.*, genetic effects on the mass-specific metabolic rate). We removed a single observation where a first-instar replicate had a $\dot{V}CO_2$ value less than zero. We also used SMATR to analyze the scaling of total lipid plus water content with dry body mass. ANOVA was used to test for the fixed effects of mtDNA, nuclear genome, larval instar, and all interactions on lactate accumulation, H_2O_2 concentration, mitochondrial physiology (State3, State4$_{ol}$, uncoupled respiration, RCR$^+$, and $\Delta\Psi_m$) and citrate synthase activity using averages across technical replicates. *Post hoc* comparisons among instars within a genotype or strain, and among genotypes or strains within instar were evaluated using Tukey HSD tests that were corrected for multiple testing.

Data availability

Stocks and strains are available upon request. Supplemental files including all phenotype data are available at FigShare. Supplemental material available at FigShare: https://doi.org/10.25386/genetics.7946795.

Results

Metabolic rate scaling with mass varies across larval instars and strains

Metabolic rate scales with mass according to the power function $R = aM^b$, where a is the constant scaling coefficient, M is mass, and b is the scaling exponent (Kleiber 1932). The scaling exponent b, estimated by the slope of the relationship between log-transformed metabolic rate and mass, differed significantly across larval instars (Figure 1A) (LR = 18.1, df = 2, P = 0.0001). Metabolic scaling with body mass was hypermetric in first-instar larvae [b (CI) = 1.42 (1.21, 1.67)], isometric in second-instar larvae [b = 1.04 (0.95, 1.15)], and hypometric in third-instar larvae [b = 0.85 (0.71, 1.01)]. Within first- and second-instar larvae, there was no evidence that metabolic scaling with mass differed significantly among strains, nor were there significant effects of strain on the elevation of the fitted relationship (*i.e.*, on the mass-specific metabolic rate) (Figure 1, B and C and Table 1). However, there was more variance among strains in mass-specific metabolic rate in first-instar larvae relative to second-instar larvae (Figure 1, B and C and Table 1). Metabolic scaling with mass in third-instar larvae differed significantly among strains, as evidenced by significantly different slopes (Figure 1D and Table 1). The variation in metabolic scaling with mass did not result from natural strains differing from mito-nuclear genotypes, but rather from variation in the scaling exponent within both groups. The pattern was significant regardless of the inclusion of several data points that, while not statistical outliers, did appear as outliers in the relationship between metabolic rate and mass (Figure 1D and Supplemental Material, Table S1).

Table 1 Ontogenetic and genetic effects on the scaling of routine metabolic rate (RMR) as a function of mass

Phenotype	Strain	Slope (95% CI)[a]	Y-intercept[b]
First-instar RMR		H_0: equal slopes (LR = 4.61, df = 5, P = 0.46)	H_0: no elevation difference ($Wald$ = 9.28, df = 5, P = 0.10)
	Common slope	1.29 (1.10, 1.54)	
	VT10		0.66 (0.54, 0.77)
	VT4		0.75 (0.64, 0.86)
	(*ore*);*Aut*		0.62 (0.51, 0.73)
	(*ore*);*OreR*		0.61 (0.43, 0.79)
	(*simw*^{501});*Aut*		0.50 (0.26, 0.75)
	(*simw*^{501});*OreR*		0.59 (0.42, 0.75)
Second-instar RMR		H_0: equal slopes (LR = 3.99, df = 5, P = 0.55)	H_0: no elevation difference ($Wald$ = 2.58, df = 5, P = 0.76)
	Common slope	1.01 (0.90, 1.13)	
	VT10		0.65 (0.55, 0.75)
	VT4		0.71 (0.6, 0.81)
	(*ore*);*Aut*		0.67 (0.58, 0.75)
	(*ore*);*OreR*		0.62 (0.51, 0.73)
	(*simw*^{501});*Aut*		0.67 (0.55, 0.79)
	(*simw*^{501});*OreR*		0.67 (0.57, 0.76)
Third-instar RMR		H_0: equal slopes (LR = 20.1, df = 5, P = 0.001)	
	VT10	1.16 (0.65, 2.06)	
	VT4	0.78 (0.54, 1.10)	
	(*ore*);*Aut*	0.81 (0.65, 1.00)	
	(*ore*);*OreR*	1.00 (0.81, 1.24)	
	(*simw*^{501});*Aut*	0.36 (0.25, 0.52)	
	(*simw*^{501});*OreR*	0.41 (0.19, 0.89)	

[a] Either strain-specific slopes or a common slope with confidence interval, when justified by the test for equal slopes among strains.
[b] In no case was there evidence that there was a shift in mass along the *x*-axis among strains ($P > 0.09$).

To get an estimate of the extent to which changes in body composition were underlying ontogenetic differences in the mass scaling of metabolic rate, we tested whether the relationship between lipid plus water content and dry mass differed among instars. Lipid and water are metabolically less active components of body mass, and we predicted that the decreased scaling of metabolic rate with mass in third-instar larvae could be the result of a greater amount of this metabolically less-active mass. We found a significant effect of instar on the *y*-intercept of the relationship between lipid plus water content and dry mass (Figure S1 and Table S2). Third-instar larvae did have greater lipid plus water content as a function of dry mass relative to second-instar larvae. However, first-instar larvae had values of this parameter similar to third-instar larvae.

Mitochondrial respiration is similar across larval instars and strains

Despite these ontogenetic and genetic differences in the scaling of organismal metabolic rate with mass, second- and third-instar larvae had similar rates of mitochondrial oxygen consumption linked to ATP production (*i.e.*, State 3 respiration) per unit of mitochondrial protein in both mito-nuclear genotypes (instar, $P = 0.13$) and natural strains (instar, $P = 0.12$) (Figure 2) (Table S3). Measures of State 3 respiration from first-instar larvae mitochondria were either below our detection limits or of low-quality, even when including similar amounts of larval mass in the preparation. This indicates that there is an increase in mitochondrial quantity or functional capacity between the first- and second-larval instars. Furthermore, larval State 3 respiration did not differ significantly among mito-nuclear genotypes or natural strains, nor were there any significant interactions between instar and genetic factors (Table S2). Maximum respiratory capacity of mitochondria (or CCCP- induced uncoupled respiration, State 3u) was also maintained across larval instars in all mito-nuclear genotypes (instar, $P = 0.18$) (Figure S1A and Table S2). However, the natural strain *VT10* had a significantly elevated maximal respiratory capacity in the second instar that resulted in a significant instar-by-genotype interaction ($P = 0.001$) (Figure S2A and Table S3).

Healthy mitochondria have high rates of oxygen consumption and ATP production when ADP is abundant (*i.e.*, State 3 respiration), but low rates of oxygen consumption in the absence of ATP synthesis (*i.e.*, State 4_{ol} respiration). The ratio of these two measures is called the respiratory control ratio (RCR^+). While the RCR^+ was generally maintained at a ratio of 2–3 across strains and instars, mitochondria of larvae from two strains, (*ore*);*OreR* and *VT10*, had elevated RCR^+ in the third instar that contributed to a significant instar-by-genotype interaction in both mito-nuclear genotypes (instar × nuclear, $P = 0.004$) and natural strains (instar × strain, $P = 0.0001$) (Figure S2B and Table S3). This was due to decreased State 4_{ol} respiration in second-instar mitochondria from these strains (Figure S2C and Table S3).

Certain genotypes and strains use anaerobic ATP production further into development

We measured the activity of citrate synthase, a nuclear-encoded enzyme located in the mitochondrial matrix. As the first step in the tricarboxylic acid (TCA) cycle, the activity of this enzyme is often used as an indicator of oxidative

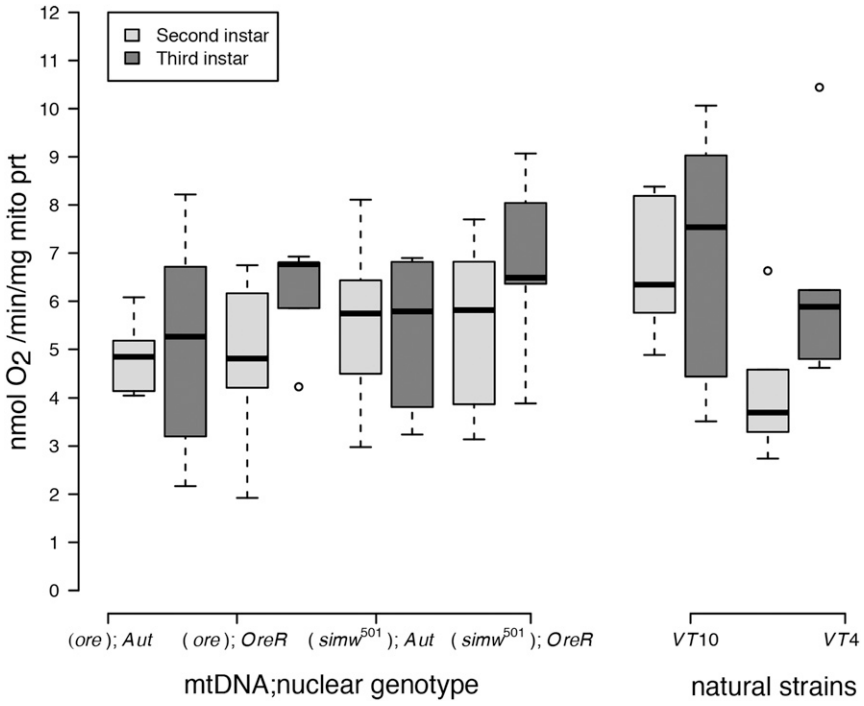

Figure 2 Oxygen-coupled ATP production, measured by the State 3 mitochondrial oxygen consumption per unit of mitochondrial protein, was maintained at statistically similar levels across strains and instars (Table S3).

capacity. Citrate synthase activity per unit of mitochondrial protein increased across development in larvae of all mito-nuclear genotypes and strains (Figure 3) (mito-nuclear genotypes: instar, $P < 0.0001$; natural strains: instar, $P < 0.0001$). There were also genotype-specific effects on citrate synthase activity. Larvae with the incompatible (*simw*^{501});*OreR* genotype had elevated citrate synthase activity relative to other genotypes across all three instars (Figure 3), resulting in significant mito-nuclear variance for this measure of oxidative capacity (mito × nuclear, $P = 0.022$) (Table S4). Interactions between instar and strain significantly affected citrate synthase activity in the natural strains, as well (instar × strain, $P = 0.010$). Larvae of particular genotypes and strains could be categorized as those for which citrate synthase reaches its maximal level by the second instar (*e.g.*, *VT10* and (*ore*); *Aut*) and those for which second-instar mitochondria have citrate synthase activity levels intermediate to first- and third-instar mitochondria [*e.g.*, *VT4* and (*ore*);*OreR*] (Figure 3).

In addition to aerobic, oxidative ATP production, *D. melanogaster* larvae use anaerobic, glycolytic ATP production that results in the production of lactate. There was significant genetic variation in the extent to which larvae accumulated lactate during development. Second-instar larvae of some strains accumulated lactate, while larvae of other strains did not accumulate any lactate across development (Figure 4A). This variation was observed within both the mito-nuclear genotypes (instar × mtDNA × nuclear, $P = 0.033$) and the natural strains (instar × strain, $P = 0.009$). Larvae with the incompatible (*simw*^{501});*OreR* genotype accumulated the highest amounts of lactate in the second instar, relative to other genotypes, resulting in a strong mito-nuclear interaction (Figure 4B and Table S5). Larvae from the natural strain *VT4* also accumulated high levels of lactate in the second instar (Figure 4A). Furthermore, larvae from strains that had intermediate levels of citrate synthase activity during the second instar [*e.g.*, *VT4* and (*ore*);*OreR*] also tended to have increased lactate accumulation during the second instar.

Larvae with a mito-nuclear incompatibility accumulated more ROS

Larvae from all strains had significantly increased levels of H_2O_2 by the third instar, relative to earlier instars ($P < 0.0001$) (Figure 5A and Table S6). However, larvae with the incompatible (*simw*^{501});*OreR* genotype had significantly elevated levels of H_2O_2 in the second instar, both relative to other strains and to first- and third-instar larvae of the same genotype. This resulted in a significant effect of the instar × mtDNA × nuclear interaction on levels of H_2O_2 ($P < 0.0001$) (Figure 5B and Table S6).

We tested whether mitochondrial membrane potential ($\Delta\Psi_m$) was disrupted in (*simw*^{501});*OreR* larvae. $\Delta\Psi_m$ provides the driving force that is utilized by complex V of OXPHOS to make ATP, and is used as an indicator of mitochondrial viability and cellular health. Larvae from all strains, except (*simw*^{501});*OreR*, maintained high levels of mitochondrial membrane potential in the second and third instar (Figure 6A and Table S6). Larvae with the incompatible (*simw*^{501});*OreR* genotype had significantly lower $\Delta\Psi_m$ relative to control genotypes in both the second and third instars. The effect of the mito-nuclear interaction on $\Delta\Psi_m$ was particularly pronounced in second-instar larvae (instar × mtDNA × nuclear $P < 0.0001$) (Figure 6B and Table S7).

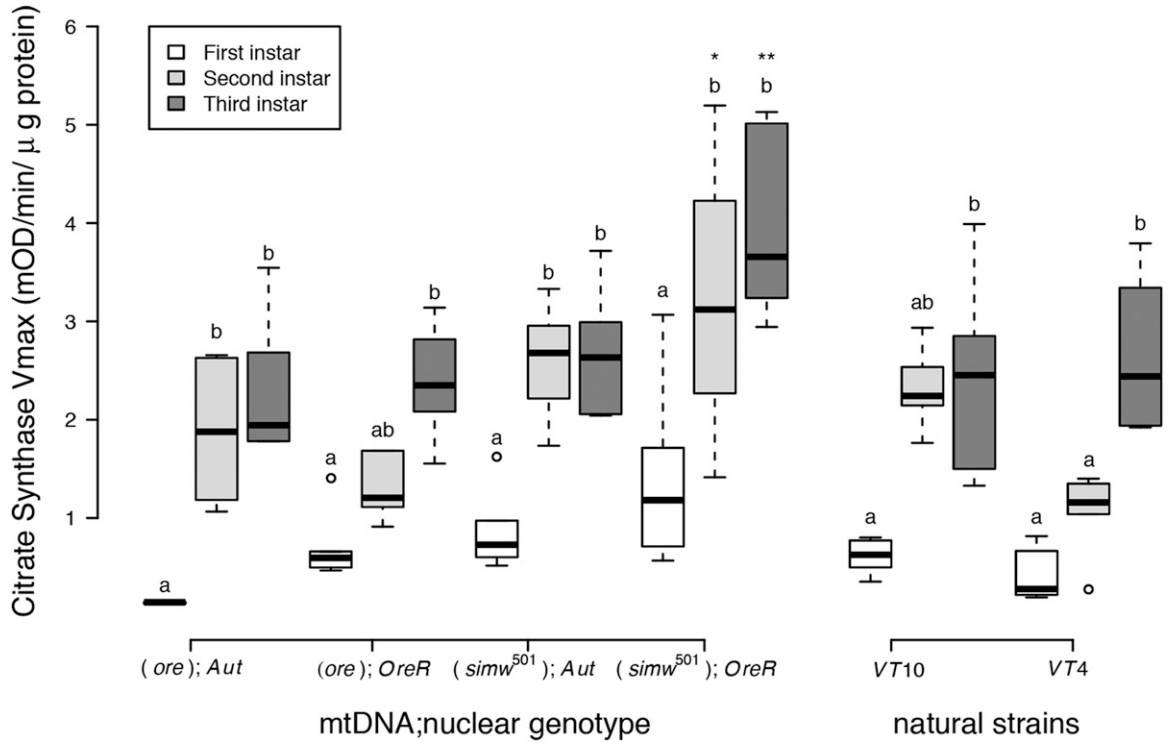

Figure 3 Oxidative capacity, measured by citrate synthase activity (V_{max}) per unit of mitochondrial protein, increased significantly across instars and was largest in larvae with the incompatible (*simw*^{501});*OreR* genotype. While larvae of all mito-nuclear genotypes increased oxidative capacity throughout development, there was significant variation among genotypes. (*simw*^{501});*OreR* larvae had significantly higher oxidative capacity than larvae with the nuclear genetic control (*ore*);*OreR* in the second (*$P_{Tukey's}$ = 0.015) and third instars (**$P_{Tukey's}$ = 0.008). The *simw*^{501} mtDNA had no effect in the *Aut* background ($P_{Tukey's} > 0.833$ in both instars), resulting in a significant mtDNA × nuclear interaction ($P = 0.022$). Natural strains from Vermont also varied significantly in the extent to which oxidative capacity reached its maximal level in the second *vs.* third instar of development (Table S4). Different letters within mito-nuclear genotypes and strains denote significantly different means at $P_{Tukey's} < 0.006$, and asterisks designate significant differences between mito-nuclear genotypes and strains of the same larval instar.

In summary, the maintenance of mitochondrial respiration in larvae with the incompatible (*simw*^{501});*OreR* genotype across second and third instars was coincident with significant increases in oxidative capacity of mitochondria, increased lactate and ROS production during the second instar, and decreased mitochondrial membrane potential, relative to larvae with control genotypes.

Discussion

Ontogenetic shifts in the relationship between metabolic rate and mass

Metabolic rates scale allometrically with mass, but the parameters that define this relationship vary among taxa, genotypes, life stages and environments (Glazier 2005; Greenlee *et al.* 2014). We found that the relationship between mass and metabolic rate differed significantly among larval instars of *D. melanogaster*. Metabolic scaling in developing animals has been described as an "impasse of principles," wherein the basic tenant of metabolic allometry—that the physiological principles of organisms are relatively conserved—is at odds with the basic tenant of development that the physiological state of organisms is dynamic across ontogeny (Burggren 2005). Insect development involves complex changes in cellular energy demand and body composition that likely affect how metabolic rate scales with mass. Thus, models and principles of interspecific allometric scaling may not be applicable to ontogenetic scaling.

We observed a shift from hypermetric scaling in first-instar larvae ($b > 1$), to isometric scaling in second-instar larvae ($b = 1$), followed by hypometric scaling in third-instar larvae ($b < 1$). This shift in metabolic scaling toward lower mass-specific metabolic rates in larger instars, was in spite of our observation that larger instars had seemingly greater oxidative capacity, as indicated by increased levels of citrate synthase activity per unit of mitochondria. Nevertheless, mitochondrial oxygen consumption linked to ATP production was maintained at similar levels across second- and third-instar larvae. These patterns suggest that although there may be increased oxidative capacity of mitochondria as development progresses, mitochondrial respiration and organismal respiration are not simple reflections of oxidative capacity, but rather are emergent properties of organellar, cellular, and organismal processes.

The ontogenetic change in metabolic scaling that we observed may reflect a change in energy demand across development as larval growth transitions from cell proliferation to

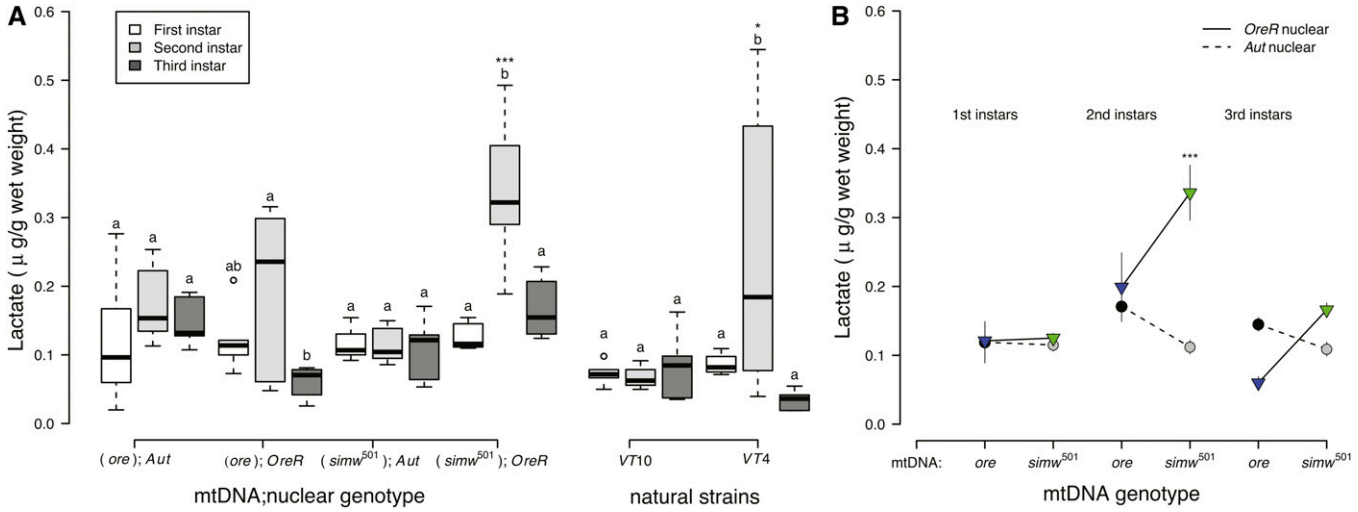

Figure 4 (A) Lactate levels per gram weight of larvae varied significantly among strains in second-instar larvae and were highest in larvae with the incompatible (*simw*^{501});*OreR* genotype. Genetic variation for second-instar larval lactate levels was also observed among natural strains from Vermont (instar × strain, $P = 0.009$) (Table S5), with *VT4* larvae having significantly more lactate than *VT10* larvae ($^{*}P_{Tukey's} = 0.014$). (B) There was a significant instar × mtDNA × nuclear interaction effect for lactate levels ($P = 0.033$) (Table S5). (*simw*^{501});*OreR* larvae had significantly higher lactate levels than did larvae from all other mito-nuclear genotypes and strains in the second instar ($^{***}P_{Tukey's} < 0.0003$). Different letters within mito-nuclear genotypes and strains denote significantly different means at $P_{Tukey's} < 0.036$, and asterisks designate significant differences between mito-nuclear genotypes and strains of the same larval instar.

cell growth. Hypermetric metabolic-scaling exponents ($b > 1$), where metabolic rates of larger individuals are greater per unit mass, could result from the increased energetic costs associated with the rapid cell proliferation and increase in cell number early in *Drosophila* development (O'Farrell 2004; Vollmer *et al.* 2017). Later in development, larval accumulation of mass occurs primarily via increases in cell volume (O'Farrell 2004), reducing the surface area to volume ratio of cells and potentially limiting metabolism. These observations support studies, collectively grouped under Resource Demand (RD) models, that suggest that metabolic scaling is driven by an intrinsic metabolic demand from the cellular level to tissue growth potential (Von Bertalanffy and Pirozynski 1953; Shin and Yasuo 1984, 1993; Ricklefs 2003; Glazier 2005). In this way, an organism's metabolic rate across development is a reflection of the potential of tissues for proliferation and growth (Ricklefs 2003). Our observations also contribute to a small, but growing, number of insect studies that support a conceptual framework where completion of growth in holometabolous insects is correlated with decreased mass-specific metabolic rates (Glazier 2005). In both the tobacco hornworm *Manduca sexta*, and the silkworm *Bombyx mori*, metabolic-scaling exponents also decrease across ontogeny (Blossman-Myer and Burggren 2010; Callier and Nijhout 2011, 2012; Sears *et al.* 2012).

Metabolic scaling with mass may also be influenced by the biochemical composition of the body. System Composition (SC) models hypothesize that ontogenetic changes in metabolic scaling reflect shifts in body composition and the relative proportions of metabolically active *vs.* inert or "sluggish" tissues (Glazier 2005; Isler and VanSchaik 2006; Greenlee *et al.* 2014). Lipid composition and storage change across development in *Drosophila*, with a net increase of metabolically inert storage lipids like triacylglycerides across development (Carvalho *et al.* 2012). While third-instar larvae in our study did have increased lipid plus water content per unit dry mass relative to second instars, first-instar larvae had values of this parameter similar to third-instar larvae. Thus, accumulating more water and lipid per unit dry mass cannot fully explain the observed pattern of increasingly hypometric metabolic scaling with mass across development. Another possibility is that changes in relative tissue sizes contribute to ontogenetic change in how metabolic rate scales with mass. In *Manduca*, the contribution of metabolically active gut tissue to the body decreases across development, which may contribute to an increasingly hypometric metabolic scaling with mass across development (Callier and Nijhout 2012).

Genetic variation in body composition across development could also underlie the genetic variation in metabolic scaling that we observed in third-instar larvae. If larvae with different genotypes differ in the degree to which they accumulate mass in the third instar via different types of energy storage, this could generate genetic variation for how metabolic rate scales with mass. Midway through the third instar, *D. melanogaster* membrane-lipid accumulation is paused, while levels of storage lipids like triacylglycerides increase (Carvalho *et al.* 2012). This suggests a transition in the third instar from metabolism supporting membrane synthesis and cell proliferation to metabolism supporting mass accumulation via lipid storage. If larvae with different genotypes vary in the timing or extent of this switch, this could contribute to the greater genetic variation for metabolic scaling that we observed in this developmental stage.

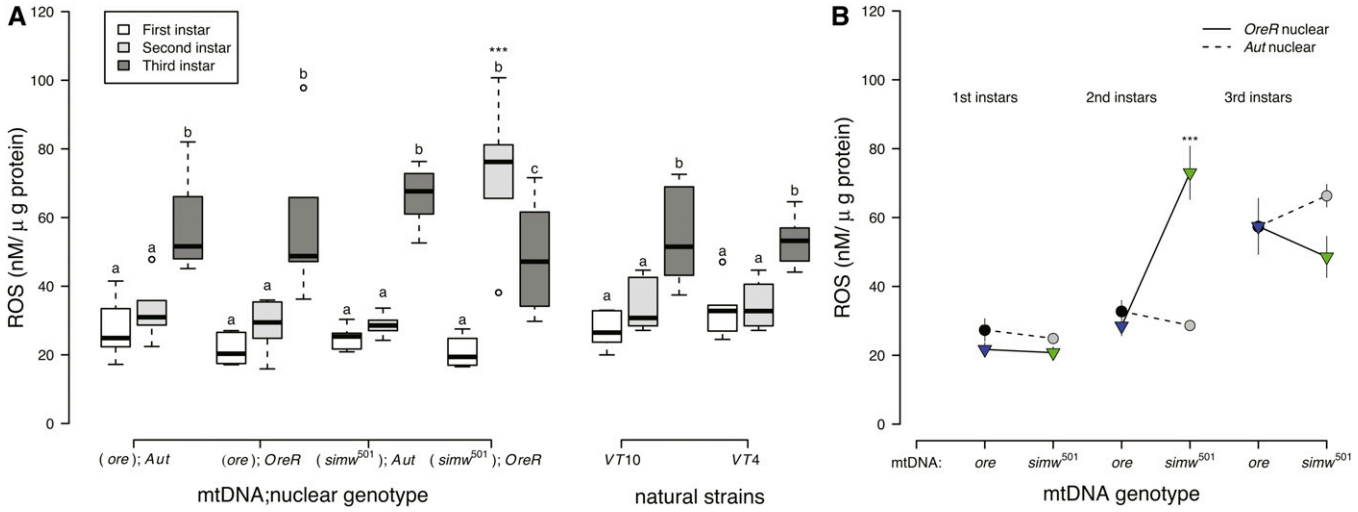

Figure 5 (A) ROS levels, measured as the concentration of H_2O_2 per gram wet weight of larvae, increased significantly across instars, and were highest in second-instar larvae with the incompatible (*simw*^{501});*OreR* genotype. (B) There was a strong effect of instar on ROS levels (instar, P = 2.347e−12), but this pattern varied among mito-nuclear genotypes (instar × mtDNA × nuclear, P = 5.166e−05) (Table S5). Second-instar (*simw*^{501});*OreR* larvae had significantly higher ROS levels relative to larvae from all other mito-nuclear genotypes (***$P_{Tukey's} < 0.0001$), while larvae from all other mito-nuclear genotypes had similar patterns of increasing ROS throughout development. The interaction between instar and strain did not affect ROS levels among larvae from natural strains (Table S5), which had a similar pattern to larvae from the control mito-nuclear genotypes. Different letters within mito-nuclear genotypes and strains denote significantly different means at $P_{Tukey's} < 0.041$, and asterisks designate significant differences between mito-nuclear genotypes and strains of the same larval instar.

Physiological compensation in larvae with a mito-nuclear incompatibility comes at a cost

Mitochondrial respiration coupled to ATP production was maintained in larvae with the mito-nuclear incompatible genotype at *in vitro* levels similar to control genotypes, despite compromised OXPHOS in flies with this genotype (Meiklejohn *et al.* 2013). The maintenance of mitochondrial respiration in these larvae was accompanied by increases in mitochondrial oxidative capacity, measured by citrate synthase activity, and glycolytic ATP production, measured by lactate accumulation, relative to larvae with control genotypes. These increases may reflect physiological compensation to maintain ATP levels in larvae whose mitochondria consume similar levels of oxygen but are less efficiently generating ATP. This compensation does not appear to occur in adult males of this genotype that have decreased mitochondrial respiration and decreased citrate synthase activity (Pichaud *et al.* 2019). We suggest that by using the functional complementation of both glycolytic and mitochondrial ATP production (*i.e.*, both substrate-level and oxidative phosphorylation), larvae of this mito-nuclear incompatible genotype are able to synthesize the ATP needed to support development.

Physiological compensation can sometimes have counterintuitive costs paid over the lifespan. While larvae with the (*simw*^{501});*OreR* genotype appear to use physiological compensation to support larval development, these larvae have significantly delayed development and compromised pupation height, immune function, and female fecundity (Meiklejohn *et al.* 2013; Zhang *et al.* 2017; Buchanan *et al.* 2018). Additionally, while *in vitro* mitochondrial respiration in larvae of this genotype was maintained similar to other strains, whole-organism metabolic rate in larvae with this genotype was elevated (Hoekstra *et al.* 2013), potentially via compensatory upregulation of citrate synthase and the TCA cycle to supply ATP. Thus, even when drawing on both glycolytic and oxidative ATP production, individuals with this mito-nuclear incompatibility may produce energy supplies very close to energetic demand. Previous results from our laboratory support this model; conditions that normally accelerate larval development, significantly magnified the developmental delay of (*simw*^{501});*OreR* larvae, suggesting that larvae with this genotype have limited capacity to compensate the defect in OXPHOS (Hoekstra *et al.* 2013, 2018). Larvae with the incompatible (*simw*^{501});*OreR* genotype may use a majority of their aerobic scope to complete normal development, limiting the resources available to allocate to other aspects of fitness. Once the demands of growth are removed, adults with this mito-nuclear incompatibility appear to regain some aerobic scope, as larvae that survived to pupation also completed metamorphosis and had normal adult size and metabolic rates (Hoekstra *et al.* 2013, 2018). However, the costs paid out during development appear to have significant impacts on adult fecundity. Both female and male fecundity were severely compromised in adults with this genotype that were developed at warmer temperatures that increase biological rates and energy demand (Hoekstra *et al.* 2013; Zhang *et al.* 2017).

At the cellular level, physiological compensation in (*simw*^{501});*OreR* larvae may be a source of oxidative stress, indicated by higher levels of H_2O_2 in larvae of this genotype, relative to other genotypes. H_2O_2 is a byproduct of the mitochondrial electron transport chain (ETC) that supports

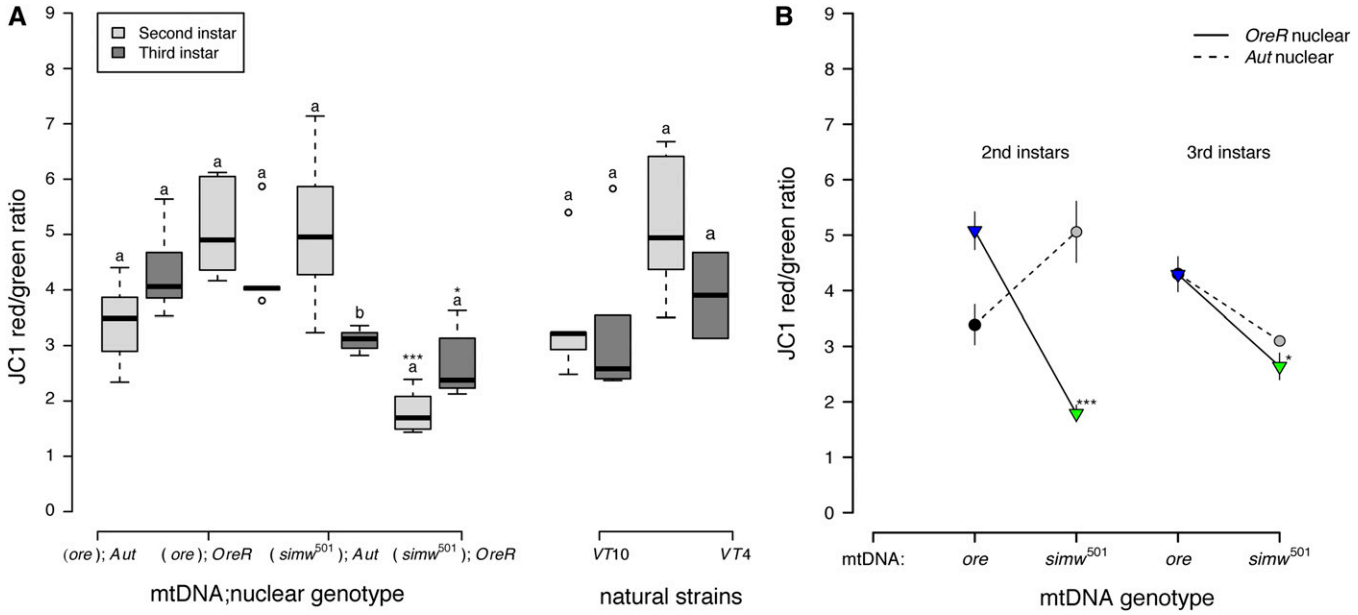

Figure 6 Larvae with the incompatible (*simw*^{501});*OreR* genotype had significantly decreased mitochondrial quality, as measured by the mitochondrial membrane potential ($\Delta\Psi_m$). (A) Both mito-nuclear control genotypes and natural strains from Vermont generally maintained high membrane potential in second- and third-instar larvae. However, (*simw*^{501});*OreR* larvae had significantly lower mitochondrial membrane potential than did larvae with the nuclear genetic control (*ore*);*OreR* in the second (***$P_{Tukey's} < 0.0001$) and third instars (*$P_{Tukey's} = 0.016$). (B) This effect of the *simw*^{501} mtDNA was not evident in the *Aut* background, where it increased membrane potential in second-instar larvae and had no effect in third-instar larvae ($P_{Tukey's} = 0.167$). This resulted in a significant instar × mtDNA × nuclear interaction effect ($P = 1.580e{-}05$) (Table S6). Values >2 typically indicate healthy mitochondria. Different letters within mito-nuclear genotypes and strains denote significantly different means at $P_{Tukey's} < 0.002$, and asterisks designate significant differences between mito-nuclear genotypes and strains of the same larval instar.

OXPHOS in healthy cells, and we observed increases in H_2O_2 as oxidative capacity increased across development in all larvae of all strains. However, compromised electron flow through the ETC can increase H_2O_2 levels and generate oxidative stress (Somero *et al.* 2017), and isolated mitochondria from adults with the mito-nuclear incompatible genotype did have higher rates of H_2O_2 production (Pichaud *et al.* 2019). There are two ways that this may be occurring. First, upregulation of the TCA cycle to supply more NADH for ATP production via the ETC may increase production of superoxide anion at Complex I. Second, there may be stoichiometric imbalance in the ETC due to presumably normal levels of cytoplasmically translated Complex II but compromised levels of the mitochondrially translated downstream OXPHOS complexes in larvae with this genotype. This could result in backflow of electrons that can produce superoxide ions when the ratio of reduced:unreduced coenzyme Q becomes elevated. The idea that individuals with the incompatible (*simw*^{501});*OreR* genotype are experiencing oxidative stress suggests an alternative interpretation of the elevated citrate synthase activity that we observed in larvae with this genotype. Levels of citrate synthase were increased in the blue mussel *Mytilus trossulus* in response to heat stress, a change that was coupled with increases in isocitrate dehydrogenase (IDH), which generates NADPH to support H_2O_2-scavenging reactions in the mitochondria (Tomanek and Zuzow 2010). This highlights the importance of considering that TCA cycle enzymes provide important functions beyond their role in OXPHOS, as they provide substrates for biosynthesis, support antioxidant reactions, and act as signaling molecules (Marden 2013; Boukouris *et al.* 2016; Somero *et al.* 2017).

Finally, we observed that mitochondria from larvae with the incompatible (*simw*^{501});*OreR* genotype could support mitochondrial oxygen consumption linked to ATP production at wild-type levels despite the fact that their membrane potential was significantly reduced. There is precedence for this observation. Mitochondrial diseases with OXPHOS defects are correlated with a suite of metabolic phenotypes that include upregulated glycolysis, lactate accumulation, elevated ROS, and decreased mitochondrial membrane potential, but stable ATP levels (Szczepanowska *et al.* 2012; Frazier *et al.* 2019). ROS act as essential secondary messengers in cellular homeostasis, but above a certain threshold level can be dangerous and lead to apoptosis (Giorgio *et al.* 2007; Bigarella *et al.* 2014). A potential defense mechanism is to decrease the mitochondrial membrane potential (*e.g.*, by uncoupling) to reduce further ROS production and protect the cell from oxidative damage (Dlasková *et al.* 2006). Our data cannot distinguish whether upregulation of citrate synthase and decreased membrane potential in the mitochondria are the cause or the consequence of oxidative stress in larvae with the mito-nuclear incompatibility. However, new models from ecophysiology (Tomanek and Zuzow 2010), developmental physiological genetic (Tennessen *et al.* 2011, 2014; Li *et al.* 2017, 2019), and disease (Ward and Thompson 2012)

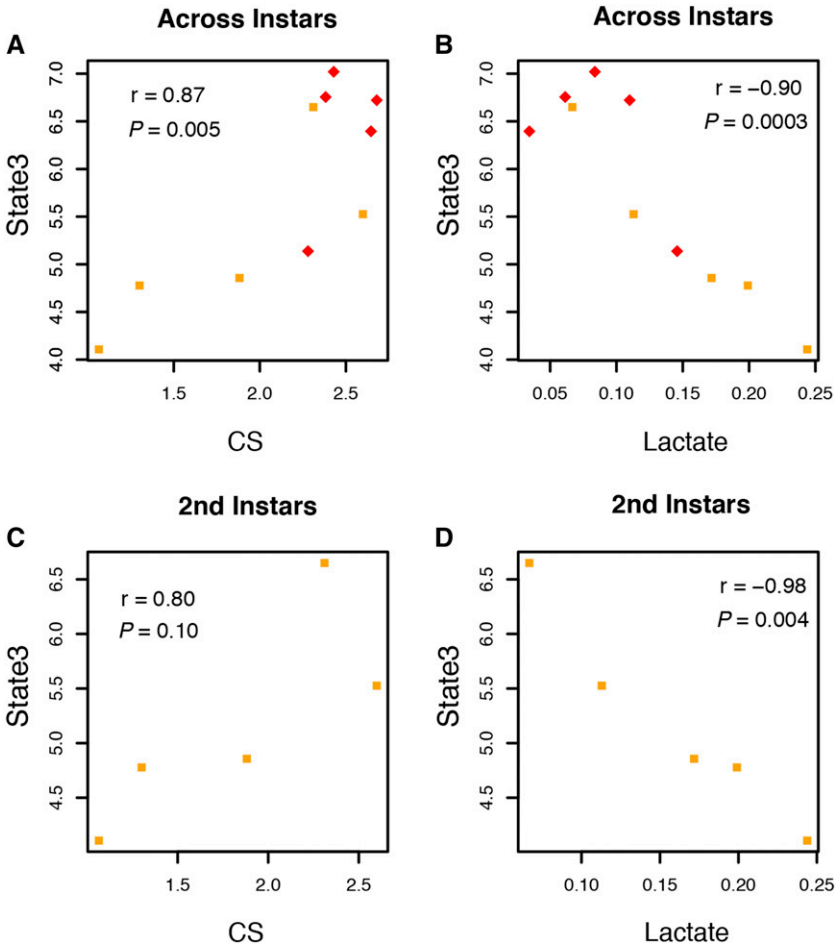

Figure 7 Components of metabolism were strongly correlated among wild-type strains, particularly in second-instar larvae. Each point represents the mean phenotype for the five wild-type strains (three mito-nuclear control genotypes and two natural strains) in second-instar (squares) and third-instar (diamonds) larvae. The Pearson's statistic *r* and associated *P* value are provided for each correlation. State 3, mitochondrial O_2 consumption linked to ATP production; CS, citrate synthase activity. (A and B) Across instars, (C and D) 2nd instars.

systems provide promising paths for future dissection of the mechanisms by which mitochondrial-nuclear genetic variation scales up to organismal fitness variation.

Genetic variation in cellular metabolism supports similar organismal outcomes

Aerobic organisms can generate ATP via mitochondrial OXPHOS, but also anaerobically via glycolytic pathways that are supported by fermentation-generated NAD^+ (*e.g.*, by lactate production). While larvae with (*simw*^{501});*OreR* genotype showed a striking pattern of both increased oxidative capacity and increased reliance on lactate metabolism, we wanted to determine the extent to which components of aerobic and anaerobic metabolism were correlated among the wild-type control and natural strains that we measured. Across instars there was a significant positive correlation between mitochondrial State 3 respiration and citrate synthase activity among wild-type strains ($r = 0.87$, $P = 0.005$), consistent with multiple aspects of oxidative capacity increasing in concert across development (Figure 7A). Within the second instar there was a similar magnitude, but nonsignificant correlation between State 3 respiration and citrate synthase activity among strains ($r = 0.8, P = 0.107$) (Figure 7C) that was not evident in the third instar ($r = 0.49$ $P = 0.406$). Thus, both aspects of oxidative metabolism increase together across development, but there is also a signature of genetic covariance for multiple aspects of oxidative metabolism within the second instar.

Across instars, there was a significant negative correlation between citrate synthase activity and lactate levels ($r = -0.87$, $P = 0.001$) and between State 3 respiration and lactate levels among strains ($r = -0.90, P = 0.0003$) (Figure 7B), consistent with high reliance on anaerobic glycolytic ATP production when oxidative capacity is low. These correlations were most evident within the second instar (CS-lactate: $r = -0.91$, $P = 0.033$, State3-lactate: $r = -0.98$, $P = 0.004$) (Figure 7D), and in the same direction, although not significant, within the third instar (CS-lactate: $r = -0.45$, $P = 0.452$, State3-lactate: $r = -0.61$, $P = 0.278$). Including traits from larvae with the (*simw*^{501}); *OreR* genotype weakened these correlations (State3-CS: $r = 0.43$, $P = 0.163$; CS-lactate: $r = -0.07$, $P = 0.829$). Thus, the mito-nuclear incompatibility breaks the genetic-physiological negative correlation between oxidative and glycolytic ATP production by significantly increasing both citrate synthase activity and lactate levels, relative to wild-type strains.

Finally, wild-type strains differed significantly in the amount of variance specifically for lactate accumulation in second instar larvae (Levene's test, $P = 0.002$). Thus, the second instar appears to be a time in development when both strains and individuals within strains differ in their reliance on glycolytic ATP production as they switch over to oxidative metabolism. This pattern is consistent with genetic variation for a metabolic switch from glycolytic to mitochondrial production of ATP regulated by the *Drosophila* estrogen-related receptor *dERR* (Tennessen and Thummel 2011; Tennessen *et al.* 2011). Yet, despite this genetic variation for how second-instar larvae generate ATP, the organismal metabolic rate of second-instar larvae appeared more robust to genetic variation than were the metabolic rates of other instars. We also observed that, despite this developmental switch from glycolytic to mitochondrial ATP production, *in vitro* mitochondrial respiration rates per unit mitochondrial protein remained constant across second- and third-instar larvae. Again, this highlights that organellar and organismal metabolic rates are not simple reflections of the underlying metabolic pathways being used. In this way, higher levels of biological organization may buffer and potentially shelter genetic variation in metabolism from selection.

dERR is responsible for a vital transcriptional switch of carbohydrate metabolism in second-instar larvae (Tennessen *et al.* 2011) that coincides with increases in lactate dehydrogenase (*dLDH*) and lactate accumulation (Li *et al.* 2017). dLDH activity recycles NAD^+ which allows for continued glycolytic ATP production and supports the TCA cycle in generating cellular building blocks to support normal cell proliferation and larval growth during development (Tennessen and Thummel 2011). Furthermore, dLDH expression and lactate production results in the accumulation of the metabolic signaling molecule L-2-hydroxyglutarate (L-2HG). L-2HG affects genome-wide DNA methylation and coordinates glycolytic flux through epigenetic modification, heterochromatin formation, and changes in gene expression (Li *et al.* 2017). We found that lactate accumulation in second-instar larvae was strongly affected by genotype, suggesting differential timing of this switch among both natural strains and mito-nuclear genotypes. Investigating potential epigenetic, bioenergetic, and life-history consequences of this genetic variation may reveal whether different metabolic strategies at the subcellular level fund similar or distinct fitness outcomes at the organismal level. This is critical for understanding whether populations harbor genetic variation in biochemical pathways that ultimately has similar fitness outcomes, or whether we should expect to see the signatures of selection acting on enzymes that control shifts in metabolic flux (*e.g.*, Flowers *et al.* 2007; Pekny *et al.* 2018).

In conclusion, the dramatic and rapid growth of *Drosophila* during ontogeny requires a precise and genetically determined metabolic program that enhances biosynthesis and proliferation coupled with a tight temporal coordination. Here, we have shown how genetic variation influence patterns of metabolism in larvae of both natural strains and mito-nuclear genotypes of *Drosophila* during developmental. Our study supports that genetic defects in core physiology can be buffered at the organismal level via physiological plasticity (Li *et al.* 2019), and that natural populations likely harbor genetic variation for distinct metabolic strategies in development that may generate similar organismal outcomes.

Acknowledgments

We would like to thank Madeleine Koenig for her assistance with sample preparation. M. Koenig was supported by the Undergraduate Creative Activities and Research Experience (UCARE) program at University of Nebraska-Lincoln (UNL). The research was supported by National Science Foundation-Integrative Organismal Systems (NSF-IOS) CAREER Award 1149178, NSF Experimental Program to Stimulate Competitive Research (EPSCoR) Track II Award 1736249, and funds from UNL to O.B.M., C.R.J., and K.L.M.

Literature Cited

Arnqvist, G., D. Dowling, E. Paul, G. Laurene, T. Tom *et al.*, 2010 Genetic architecture of metabolic rate: environment specific epistasis between mitochondrial and nuclear genes in an insect. Evolution. 64: 3354–3363. https://doi.org/10.1111/j.1558-5646.2010.01135.x

Aw, W., R. Bajracharya, S. Towarnicki, and J. Ballard, 2016 Assessing bioenergetic functions from isolated mitochondria in. J. Biol. Methods 3: e42. https://doi.org/10.14440/jbm.2016.112

Ballard, W., and D. Rand, 2005 The population biology of mitochondrial DNA and its phylogenetic implications. Annu. Rev. Ecol. Evol. Syst. 36: 621–642. https://doi.org/10.1146/annurev.ecolsys.36.091704.175513

Barabási, A., and Z. Oltvai, 2004 Network biology: understanding the cell's functional organization. Nat. Rev. Genet. 5: 101–113. https://doi.org/10.1038/nrg1272

Bigarella, C., R. Liang, and S. Ghaffari, 2014 Stem cells and the impact of ROS signaling. Development 141: 4206–4218. https://doi.org/10.1242/dev.107086

Bligh, E. G., and W. J. Dyer, 1959 A rapid method of total lipid extraction and purification. Can. J. Biochem. Physiol. 37: 911–917. https://doi.org/10.1139/y59-099

Blossman-Myer, B., and W. Burggren, 2010 Metabolic allometry during development and metamorphosis of the silkworm *Bombyx mori*: analyses, patterns, and mechanisms. Physiol. Biochem. Zool. 83: 215–231. https://doi.org/10.1086/648393

Boukouris, A., S. Zervopoulos, and E. Michelakis, 2016 Metabolic enzymes moonlighting in the nucleus: metabolic regulation of gene transcription. Trends Biochem. Sci. 41: 712–730. https://doi.org/10.1016/j.tibs.2016.05.013

Brand, M. D., L. F. Chien, E. K. Ainscow, D. F. Rolfe, and R. K. Porter, 1994 The causes and functions of mitochondrial proton leak. Biochim. Biophys. Acta 1187: 132–139. https://doi.org/10.1016/0005-2728(94)90099-X

Buchanan, J., C. Meiklejohn, and K. Montooth, 2018 Mitochondrial dysfunction and infection generate immunity-fecundity tradeoffs in *Drosophila*. Integr. Comp. Biol. 58: 591–603. https://doi.org/10.1093/icb/icy078

Burggren, W., 2005 Developing animals flout prominent assumptions of ecological physiology. Comp. Biochem. Physiol. A Mol. Integr. Physiol. 141: 430–439. https://doi.org/10.1016/j.cbpb.2005.03.010

Callier, V., and F. Nijhout, 2011 Control of body size by oxygen supply reveals size-dependent and size-independent mechanisms of molting and metamorphosis. Proc. Natl. Acad. Sci. USA 108: 14664–14669. https://doi.org/10.1073/pnas.1106556108

Callier, V., and H. F. Nijhout, 2012 Supply-side constraints are insufficient to explain the ontogenetic scaling of metabolic rate in the tobacco hornworm, Manduca sexta. *PLoS One* 7: e45455.

Callier, V., S. Hand, J. Campbell, T. Biddulph, and J. Harrison, 2015 Developmental changes in hypoxic exposure and responses to anoxia in *Drosophila melanogaster*. J. Exp. Biol. 218: 2927–2934. https://doi.org/10.1242/jeb.125849

Carvalho, M., J. Sampaio, W. Palm, M. Brankatschk, S. Eaton *et al.*, 2012 Effects of diet and development on the *Drosophila* lipidome. Mol. Syst. Biol. 8: 600. https://doi.org/10.1038/msb.2012.29

Chance, B., and G. Williams, 1955 Respiratory enzymes in oxidative phosphorylation: I. kinetics of oxygen utilization. J. Biol. Chem. 217: 383–394.

Charlesworth, B., and D. Charlesworth, 2016 Population genetics from 1966 to 2016. Heredity 118: 2–9. https://doi.org/10.1038/hdy.2016.55

Church, R., and F. Robertson, 1966 A biochemical study of the growth of *Drosophila melanogaster*. J. Exp. Zool. 162: 337–351. https://doi.org/10.1002/jez.1401620309

Clark, A., and L. Wang, 1997 Epistasis in measured genotypes: *Drosophila* p-element insertions. Genetics 147: 157–163.

Clark, A., L. Wang, and T. Hulleberg, 1995a P-element-induced variation in metabolic regulation in *Drosophila*. Genetics 139: 337–348.

Clark, A., L. Wang, and T. Hulleberg, 1995b Spontaneous mutation rate of modifiers of metabolism in *Drosophila*. Genetics 139: 767–779.

Cooper, B. S., L. A. Hammad, and K. L. Montooth, 2014 Thermal adaptation of cellular membranes in natural populations of *Drosophila melanogaster*. Funct. Ecol. 28: 886–894. https://doi.org/10.1111/1365-2435.12264

Crawford, D., and M. Oleksiak, 2007 The biological importance of measuring individual variation. J. Exp. Biol. 210: 1613–1621. https://doi.org/10.1242/jeb.005454

Dlasková, A., T. Špaček, E. Škobisová, J. Šantorová, and P. Ježek, 2006 Certain aspects of uncoupling due to mitochondrial uncoupling proteins in vitro and in vivo. Biochim. Biophys. Acta 1757: 467–473. https://doi.org/10.1016/j.bbabio.2006.05.005

Estabrook, R., 1967 Mitochondrial respiratory control and the polarographic measurement of ADP : O ratios. Methods Enzymol. 10: 41–47. https://doi.org/10.1016/0076-6879(67)10010-4

Flowers, J., E. Sezgin, S. Kumagai, D. Duvernell, L. Matzkin *et al.*, 2007 Adaptive evolution of metabolic pathways in *Drosophila*. Mol. Biol. Evol. 24: 1347–1354. https://doi.org/10.1093/molbev/msm057

Frazier, A., D. R. Thorburn, and A. G. Compton, 2019 Mitochondrial energy generation disorders: genes, mechanisms, and clues to pathology. J. Biol. Chem. 294: 5386–5395

Gefen, E., A. J. Marlon, and A. E. Gibbs, 2006 Selection for desiccation resistance in adult *Drosophila melanogaster* affects larval development and metabolite accumulation. J. Exp. Biol. 209: 3293–3300. https://doi.org/10.1242/jeb.02397

Gillespie, J., 1999 The role of population size in molecular evolution. Theor. Popul. Biol. 55: 145–156. https://doi.org/10.1006/tpbi.1998.1391

Giorgio, M., M. Trinei, E. Migliaccio, and P. Pelicci, 2007 Hydrogen peroxide: a metabolic by-product or a common mediator of ageing signals? Nat. Rev. Mol. Cell Biol. 8: 722–728. https://doi.org/10.1038/nrm2240

Glazier, D., 2005 Beyond the '3/4-power law': variation in the intra- and interspecific scaling of metabolic rate in animals. Biol. Rev. Camb. Philos. Soc. 80: 611–662. https://doi.org/10.1017/S1464793105006834

Glazier, D., 2014 Metabolic scaling in complex living systems. Systems 2: 451–540. https://doi.org/10.3390/systems2040451

Glazier, D. S., 2015 Is metabolic rate a universal 'pacemaker' for biological processes? Biol. Rev. Camb. Philos. Soc. 90: 377–407. https://doi.org/10.1111/brv.12115

Graveley, B. R., A. N. Brooks, J. W. Carlson, M. O. Duff, J. M. Landolin *et al.*, 2011 The developmental transcriptome of *Drosophila melanogaster*. Nature 471: 473–479. https://doi.org/10.1038/nature09715

Greenlee, K., K. Montooth, and B. Helm, 2014 Predicting performance and plasticity in the development of respiratory structures and metabolic systems. Integr. Comp. Biol. 54: 307–322. https://doi.org/10.1093/icb/icu018

Harris, H., 1966 Genetics of man enzyme polymorphisms in man. Proc. R. Soc. Lond. B. Biol. Sci. 164: 298–310.

Hoekstra, L., M. Siddiq, and K. Montooth, 2013 Pleiotropic effects of a mitochondrial–nuclear incompatibility depend upon the accelerating effect of temperature in *Drosophila*. Genetics 195: 1129–1139. https://doi.org/10.1534/genetics.113.154914

Hoekstra, L. A., C. R. Julick, K. M. Katelyn, and K. L. Montooth, 2018 Energy demand and the context-dependent effects of genetic interactions underlying metabolism. Evol. Lett. 2: 102–113. https://doi.org/10.1002/evl3.47

Holmbeck, M., J. Donner, E. Villa-Cuesta, and D. Rand, 2015 A *Drosophila* model for mito-nuclear diseases generated by an incompatible interaction between tRNA and tRNA synthetase. Dis. Model. Mech. 8: 843–854. https://doi.org/10.1242/dmm.019323

Hubby, J., and R. Lewontin, 1966 A molecular approach to the study of genic heterozygosity in natural populations. I. the number of alleles at different loci in *Drosophila pseudoobscura*. Genetics 54: 577–594.

Isler, K., and C. VanSchaik, 2006 Metabolic costs of brain size evolution. Biol. Lett. 2: 557–560. https://doi.org/10.1098/rsbl.2006.0538

Jeong, H., B. Tombor, R. Albert, Z. Oltvai, and A. Barabási, 2000 The large-scale organization of metabolic networks. Nature 407: 651–654. https://doi.org/10.1038/35036627

Kimura, M., 1983 *The Neutral Theory of Molecular Evolution*. Cambridge University Press, Cambridge. https://doi.org/10.1017/CBO9780511623486

Kleiber, M., 1932 Body size and metabolism. Hilgardia 6: 315–353. https://doi.org/10.3733/hilg.v06n11p315

Kurbalija Novičić, Z., E. Immonen, M. Jelić, M. Anđelković, M. Stamenković-Radak *et al.*, 2015 Within-population genetic effects of mtDNA on metabolic rate in *Drosophila subobscura*. J. Evol. Biol. 28: 338–346. https://doi.org/10.1111/jeb.12565

Laurie-Ahlberg, C., G. Maroni, G. Bewley, J. Lucchesi, and B. Weir, 1980 Quantitative genetic variation of enzyme activities in natural populations of *Drosophila melanogaster*. Proc. Natl. Acad. Sci. USA 77: 1073–1077. https://doi.org/10.1073/pnas.77.2.1073

Laurie-Ahlberg, C., A. Wilton, J. Curtsinger, and T. Emigh, 1982 Naturally occurring enzyme activity variation in *Drosophila melanogaster*. I. sources of variation for 23 enzymes. Genetics 102: 191–206.

Lewontin, R., and J. Hubby, 1966 A molecular approach to the study of genic heterozygosity in natural populations. II. amount of variation and degree of heterozygosity in natural populations of *Drosophila pseudoobscura*. Genetics 54: 595–609.

Li, H., G. Chawla, A. Hurlburt, M. Sterrett, O. Zaslaver *et al.*, 2017 *Drosophila* larvae synthesize the putative oncometabolite L-2-hydroxyglutarate during normal developmental growth. Proc. Natl. Acad. Sci. USA 114: 1353–1358. https://doi.org/10.1073/pnas.1614102114

Li, H., K. Buddika, M. C. Sterrett, C. R. Julick, R. C. Pletcher *et al.*, 2019 Lactate and glycerol-3-phosphate metabolism cooperatively regulate growth and redox balance during *Drosophila melanogaster* larval development. bioRxiv: 517532.https://doi.org/10.1101/517532

Marden, J., 2013 Nature's inordinate fondness for metabolic enzymes: why metabolic enzyme loci are so frequently targets of selection. Mol. Ecol. 22: 5743–5764. https://doi.org/10.1111/mec.12534

Martin, A., 1995 Metabolic rate and directional nucleotide substitution in animal mitochondrial DNA. Mol. Biol. Evol. 12: 1124–1131.

Meiklejohn, C., and D. Hartl, 2002 A single mode of canalization. Trends Ecol. Evol. 17: 468–473. https://doi.org/10.1016/S0169-5347(02)02596-X

Meiklejohn, C., M. Holmbeck, M. Siddiq, D. Abt, D. Rand *et al.*, 2013 An incompatibility between a mitochondrial tRNA and its nuclear-encoded tRNA synthetase compromises development and fitness in *Drosophila*. PLoS Genet. 9: e1003238. https://doi.org/10.1371/journal.pgen.1003238

Miettinen, T., and M. Björklund, 2017 Mitochondrial function and cell size: an allometric relationship. Trends Cell Biol. 27: 393–402. https://doi.org/10.1016/j.tcb.2017.02.006

Mitchell-Olds, T., and D. Pedersen, 1998 The molecular basis of quantitative genetic variation in central and secondary metabolism in *Arabidopsis*. Genetics 149: 739–747.

Montooth, K. L., J. H. Marden, and A. G. Clark, 2003 Mapping determinants of variation in energy metabolism, respiration and flight in *Drosophila*. Genetics 165: 623–635.

Montooth, K. L., C. D. Meiklejohn, D. N. Abt, and D. M. Rand, 2010 Mitochondrial-nuclear epistasis affects fitness within species but does not contribute to fixed incompatibilities between species of *Drosophila*. Evolution 64: 3364–3379. https://doi.org/10.1111/j.1558-5646.2010.01077.x

Munro, D., and J. R. Treberg, 2017 A radical shift in perspective: mitochondria as regulators of reactive oxygen species. J. Exp. Biol. 220: 1170–1180. https://doi.org/10.1242/jeb.132142

Nespolo, R., L. Castañeda, and D. Roff, 2007 Quantitative genetic variation of metabolism in the nymphs of the sand cricket, *Gryllus firmus*, inferred from an analysis of inbred-lines. Biol. Res. 40: 5–12. https://doi.org/10.4067/S0716-97602007000100001

O'Farrell, P., 2004 How metazoans reach their full size: the natural history of bigness, pp. 1–22 in *Cell Growth: Control of Cell Size*, edited by M. Hall, M. Raff, and G. Thomas. Cold Spring Harbor Laboratory Press, New York.

Pekny, J. E., P. B. Smith, and J. H. Marden, 2018 Enzyme polymorphism, oxygen and injury: a lipidomic analysis of flight-induced oxidative damage in a succinate dehydrogenase d (Sdhd)-polymorphic insect. J. Exp. Biol. 221: pii: jeb171009. https://doi.org/10.1242/jeb.171009

Pichaud, N., R. Bérubé, G. Côté, C. Belzile, F. Dufresne *et al.*, 2019 Age dependent dysfunction of mitochondrial and ROS metabolism induced by mitonuclear mismatch. Front. Genet. 10: 130. https://doi.org/10.3389/fgene.2019.00130

Porter, R., and M. Brand, 1993 Body mass dependence of H^+ leak in mitochondria and its relevance to metabolic rate. Nature 362: 628–630. https://doi.org/10.1038/362628a0

Porter, R., A. Hulbert, and M. Brand, 1996 Allometry of mitochondrial proton leak: influence of membrane surface area and fatty acid composition. Am. J. Physiol. Integr. Comp. Physiol. 271: R1550–R1560. https://doi.org/10.1152/ajpregu.1996.271.6.R1550

R Development Core Team 2011 R: a language and environment for statistical computing. R Foundation for Statistical Computing, Vienna, Austria.

Ravasz, E., A. Somera, D. Mongru, Z. Oltvai, and A. Barabási, 2002 Hierarchical organization of modularity in metabolic networks. Science 297: 1551–1555. https://doi.org/10.1126/science.1073374

Ricklefs, R., 2003 Is rate of ontogenetic growth constrained by resource supply or tissue growth potential? A comment on West *et al.*'s model. Funct. Ecol. 17: 384–393. https://doi.org/10.1046/j.1365-2435.2003.00745.x

Sears, K., A. Kerkhoff, A. Messerman, and H. Itagaki, 2012 Ontogenetic scaling of metabolism, growth, and assimilation: testing metabolic scaling theory with *Manduca sexta* larvae. Physiol. Biochem. Zool. 85: 159–173. https://doi.org/10.1086/664619

Shin, O., and I. Yasuo, 1984 Allometric relationship between tissue respiration and body mass in the carp. Comp. Biochem. Physiol. A Mol. Integr. Physiol. 77: 415–418. https://doi.org/10.1016/0300-9629(84)90205-6

Shin, O., and I. Yasuo, 1993 Allometric relationship between tissue respiration and body mass in a marine teleost, porgy *Pagrus major*. Comp. Biochem. Physiol. A Mol. Integr. Physiol. 105: 129–133.

Somero, G., B. Lockwood, and L. Tomanek, 2017 *Biochemical Adaptation: Response to Environmental Challenges, from Life's Origins to the Anthropocene*. Sinauer Associates, Sunderland, MA

Strogatz, S. H., 2001 Exploring complex networks. Nature 410: 268–276. https://doi.org/10.1038/35065725

Szczepanowska, J., D. Malinska, M. Wieckowski, and J. Duszynski, 2012 Effect of mtDNA point mutations on cellular bioenergetics. Biochim. Biophys. Acta 1817: 1740–1746. https://doi.org/10.1016/j.bbabio.2012.02.028

Tennessen, J., K. Baker, G. Lam, J. Evans, and C. Thummel, 2011 The *Drosophila* estrogen-related receptor directs a metabolic switch that supports developmental growth. Cell Metab. 13: 139–148. https://doi.org/10.1016/j.cmet.2011.01.005

Tennessen, J. M., and C. S. Thummel, 2011 Coordinating growth and review maturation — insights from *Drosophila*. Curr. Biol. 21: R750–R757. https://doi.org/10.1016/j.cub.2011.06.033

Tennessen, J. M., N. M. Bertagnolli, J. Evans, M. H. Sieber, J. Cox *et al.*, 2014 Coordinated metabolic transitions during Drosophila embryogenesis and the onset of aerobic glycolysis. G3 (Bethesda) 4: 839–850. https://doi.org/10.1534/g3.114.010652

Tieleman, I., M. Versteegh, A. Fries, B. Helm, N. Dingemanse *et al.*, 2009 Genetic modulation of energy metabolism in birds through mitochondrial function. Proc. R. Soc. B Biol. Sci. 276: 1685–1693.

Tishkoff, S. A., R. Varkonyi, N. Cahinhinan, S. Abbes, G. Argyropoulos *et al.*, 2001 Haplotype diversity and linkage disequilibrium at human G6PD: recent origin of alleles that confer malarial resistance. Science 293: 455–462. https://doi.org/10.1126/science.1061573

Tomanek, L., and M. Zuzow, 2010 The proteomic response of the mussel congeners *Mytilus galloprovincialis* and *M. trossulus* to acute heat stress: implications for thermal tolerance limits and metabolic costs of thermal stress. J. Exp. Biol. 213: 3559–3574. https://doi.org/10.1242/jeb.041228

Van Dyken, J. D., and M. J. Wade, 2010 The genetic signature of conditional expression. Genetics 184: 557–570. https://doi.org/10.1534/genetics.109.110163

Verrelli, B., and W. Eanes, 2001 The functional impact of Pgm amino acid polymorphism on glycogen content in *Drosophila melanogaster*. Genetics 159: 201–210.

Villa-Cuesta, E., M. Holmbeck, and D. Rand, 2014 Rapamycin increases mitochondrial efficiency by mtDNA-dependent reprogramming of mitochondrial metabolism in *Drosophila*. J. Cell Sci. 127: 2282–2290. https://doi.org/10.1242/jcs.142026

Vollmer, J., F. Casares, and D. Iber, 2017 Growth and size control during development. Open Biol. 7: pii: 170190. https://doi.org/10.1098/rsob.170190

Von Bertalanffy, L., and W. Pirozynski, 1953 Tissue respiration, growth, and basal metabolism. Biol. Bull. 105: 240–256. https://doi.org/10.2307/1538640

Waddington, C., 1942 Canalization of development and the inheritance of acquired characters. Nature 150: 563–565. https://doi.org/10.1038/150563a0

Waddington, C., 1957 *The Strategy of the Genes: A Discussion of Some Aspects of Theoretical Biology*. George Allen & Unwin, Ltd., London.

Ward, P. S., and C. B. Thompson, 2012 Signaling in control of cell growth and metabolism. Cold Spring Harb. Perspect. Biol. 4: a006783. https://doi.org/10.1101/cshperspect.a006783

Warton, D., I. Wright, D. Falster, and M. Westoby, 2006 Bivariate line-fitting methods for allometry. Biol. Rev. Camb. Philos. Soc. 81: 259–291. https://doi.org/10.1017/S1464793106007007

Watt, W., 1977 Adaptation at specific loci. I. natural selection on phosphogluco isomerase of *Colias* butterflies: biochemical and population aspects. Genetics 87: 177–194.

Watt, W., R. Cassin, and M. Swan, 1983 Adaptation at specific loci. III. field behavior and survivorship differences among *Colias* PGI genotypes are predictable from in vitro biochemistry. Genetics 103: 725–739.

Watt, W., C. Wheat, E. Meyer, and J. Martin, 2003 Adaptation at specific loci. VII. natural selection, dispersal and the diversity of molecular–functional variation patterns among butterfly species complexes (*Colias*: Lepidoptera, Pieridae). Mol. Ecol. 12: 1265–1275. https://doi.org/10.1046/j.1365-294X.2003.01804.x

Zhang, C., K. Montooth, and B. Calvi, 2017 Incompatibility between mitochondrial and nuclear genomes during oogenesis results in ovarian failure and embryonic lethality. Development 144: 2490–2503. https://doi.org/10.1242/dev.151951

Communicating editor: M. Wolfner